NIH Public Access
Author Manuscript
Arterioscler Thromb Vasc Biol. Author manuscript; available in PMC 2013 May 09.

Published in final edited form as:
Arterioscler Thromb Vasc Biol. 2012 January ; 32(1): 65–73. doi:10.1161/ATVBAHA.111.239137.

Disruption of Endothelial Peroxisome Proliferator-activated Receptor γ Accelerates Diet-induced Atherogenesis in Low-density Lipoprotein Receptor-null Mice

Aijuan Qu, **Yatrik M. Shah**, **Soumen K. Manna**, and **Frank J. Gonzalez**
Laboratory of Metabolism, Center for Cancer Research, National Cancer Institute, National Institutes of Health, Bethesda, MD 20892 (A.Q, Y.M.S, S.K.M., F.J.G.); Department of Molecular and Integrative Physiology and Internal Medicine, Division of Gastroenterology, University of Michigan School of Medicine, Ann Arbor, MI 48109 (Y.M.S.)

Abstract

Objective—Peroxisome proliferator-activated receptor γ (PPARγ) is widely expressed in vessel walls, and its activation by agonists showed beneficial effects in cardiovascular diseases. However, the role of endothelial cell (EC) PPARγ in atherogenesis is not fully understood.

Methods and Results—To assess the contribution of endothelial-specific PPARγ in atherosclerosis, EC-specific PPARγ disruption and low-density lipoprotein receptor (LDLR) double-knockout ($Ppar\gamma^{\Delta EC}/Ldlr^{-/-}$) mice were developed. When challenged with a high-cholesterol diet for 4 weeks, $Ppar\gamma^{\Delta EC}/Ldlr^{-/-}$ mice exhibited severe atherosclerotic lesions compared to either their littermate controls or macrophage-specific PPARγ disruption and low-density lipoprotein receptor (LDLR) double knockout ($Ppar\gamma^{\Delta M\phi}/Ldlr^{-/-}$) mice. Metabolic analysis showed severe dyslipidemia and significant increase in systolic blood pressure in the $Ppar\gamma^{\Delta M\phi}/Ldlr^{-/-}$ mice. Histological analysis and real-time quantitative PCR suggested an exacerbated inflammation in $Ppar\gamma^{\Delta EC}/Ldlr^{-/-}$ mice, as revealed by the increases of proinflammatory gene expression and macrophage infiltration *in vivo* and *in vitro*. Furthermore, *in vivo* endothelial permeability was also increased by endothelial PPARγ disruption. Bone-marrow transplantation studies, which reconstituted hematopoietic PPARγ, demonstrated that the accelerated atherogenesis was due to endothelial PPARγ deficiency.

Conclusions—Endothelial PPARγ plays an important protective role in atherogenesis.

Keywords

atherosclerosis; endothelium; PPARγ; inflammation

Introduction

Peroxisome proliferators-activated receptor γ (PPARγ) is a ligand-activated nuclear transcription factor that has a central role in controlling adipocyte differentiation, lipid metabolism, and insulin sensitivity [1]. Clinically, PPARγ agonists, thiazolidinedione (TZD) class of drugs are used to improve insulin resistance and treat type 2 diabetes. PPARγ is also highly expressed in endothelial cells (EC), macrophages (Mϕ), and smooth muscle cells, all of which are critical in atherosclerosis. Several studies have shown that TZD

Correspondence to Frank J. Gonzalez, Building 37, Room 3106, National Institutes of Health, Bethesda, MD 20814 (gonzalef@mail.nih.gov).

Disclosures
None.

NIH-PA Author Manuscript
NIH-PA Author Manuscript
NIH-PA Author Manuscript

NIH-PA Author Manuscript

NIH-PA Author Manuscript

NIH-PA Author Manuscript

administration reduces atherosclerosis in both apolipoprotein E ($ApoE$)$^{-/-}$ and low-density lipoprotein receptor ($Ldlr$)$^{-/-}$ mice[2–4]. Recently, a conditional disruption of PPARγ in macrophages demonstrated an increase in atherosclerosis under conditions of mild and severe hypercholesterolemia[5]. Moreover, disruption of PPARγ in smooth muscle cells augments Angiotensin-II induced atherosclerosis in $Ldlr^{-/-}$ mice[6] and exacerbates vascular lesion formation[7].

Endothelial cell activation and dysfunction upon exposure to atheroprone factors, such as oxidized lipids and proinflammatory stimuli play a critical role in the initiation and progression of atherosclerosis[8, 9]. Increasing data have shown that PPARγ agonists inhibit inflammation in endothelial cells and suppress the expression of vasoconstrictors endothelin-1 and angiotensin-II, but enhance the expression and activity of vasodilator nitric oxide in cultured ECs [10–14]. Since PPARγ agonists demonstrate receptor-independent functions the direct role of PPARγ in endothelial cells remains unknown. Moreover, in the PROACTIVE trial, the PPARγ agonist pioglitazone had beneficial effects on cardiovascular diseases[15], but a recent meta-analysis demonstrates that PPARγ agonist rosiglitazone was associated with an increase in risk of myocardial infarction and a trend toward a higher risk of cardiovascular death in patients with type 2 diabetes[16]. These clinical trials raise the importance of understanding the role of PPARγ in cell types critical in the progression of cardiovascular diseases.

In the present study, EC-specific PPARγ deficient mice were generated using Cre/loxP system regulated by the Tie2 promoter on the $Ldlr^{-/-}$ background. The data demonstrate that PPARγ deficiency in ECs significantly accelerates the initiation of atherosclerosis in $Ldlr^{-/-}$ mice challenged with an atherogenic diet, demonstrating a protective role of endothelial PPARγ against the initiation and development of atherosclerosis.

Methods and Materials

Animals and Diets

$Pparγ^{F/F}$ [17], $Pparγ^{ΔEC}$ [18, 19] and $Pparγ^{ΔMϕ}$ [20] mice were previously described. $Ldlr^{-/-}$ mice on C57BL/6 background were purchased from Jackson Laboratories Inc (Bar Harbor, Me). $Pparγ^{ΔEC}$ and $Pparγ^{ΔMϕ}$ mice were crossed with $Ldlr^{-/-}$ mice to obtain $Pparγ^{ΔEC}/Ldlr^{-/-}$ and $Pparγ^{ΔMϕ}/Ldlr^{-/-}$ mice and the littermate $Pparγ^{F/F}/Ldlr^{-/-}$ were used as controls for all studies. All mice were maintained in micro-isolator cages with free access to rodent chow and water. Atherosclerosis was induced by feeding male mice an atherogenic rodent diet containing 1.25% cholesterol and 0.5% cholic acid (TD 02028, Harlan Teklad, Madison, WI) from 6 weeks old for the indicated times. All animal studies were carried out in accordance with Institute of Laboratory Animal Resources guidelines and approved by the National Cancer Institute Animal Care and Use Committee.

Serum Lipids and Lipoprotein Profiles

Mice were fasted overnight before blood sample collection. Total serum cholesterol and triglycerides were measured using kits from Wako (Wako Chemicals USA Inc, Richmond, VA) according to the manufacture's instructions. Lipoprotein profile was assessed by fast performance liquid chromatography (FPLC) using a Superose 6 column (Pharmacia, Piscataway, NJ) on a high-performance liquid chromatography system model 600 (Waters, Milford, MA)[21, 22].

Blood Pressure Measurement

Systolic BP was analyzed by tail-cuff plethysmography on conscious (nonanesthetized) mice using BP-2000 blood pressure analysis system (Visitech Systems, Apex, NC). All mice

NIH-PA Author Manuscript

NIH-PA Author Manuscript

NIH-PA Author Manuscript

were trained on the apparatus for one week before the start of recording. Blood pressure was assessed in the morning and values were derived as an average of ten independent measurements. One complete cycle was performed before recording to allow the mice to acclimate before actual readings were taken.

Bone Marrow Transplantation (BMT)

Six-week-old male *Pparγ*$^{F/F}$/*Ldlr*$^{-/-}$ and *Pparγ*$^{\Delta EC}$/*Ldlr*$^{-/-}$ mice were lethally irradiated with 9.5 Gy from a cesium gamma source 6 hr before transplantation. The ^{137}Cs source was in a Mark I Model 68 small animal irradiator (J. L. Shepherd & Associates, San Fernando, CA) operating at 2.57 Gy/min. This unit has a single ^{137}Cs source and provides uniform doses to small animals centered on the revolving turntable revolving at a constant rate of 4.75 revolutions per minute within the chamber. Bone marrow was collected from femurs of donor *Pparγ*$^{F/F}$/*Ldlr*$^{-/-}$ or *Pparγ*$^{\Delta EC}$/*Ldlr*$^{-/-}$ mice by flushing with sterile medium (RPMI 1640, 5 U/ml heparin, 50 U/ml penicillin and 50 μg/ml streptomycin). Each recipient mouse was injected with 5×10^6 bone marrow cells through the tail vein. Four weeks after BMT, peripheral blood was collected for PCR analysis of bone marrow reconstitution[23, 24]. For atherosclerosis study, the mice were fed with high-cholesterol diet for another 4 weeks after confirming the mice were fully chimeric.

Analysis of Atherosclerotic Lesions

After 4 weeks of high cholesterol diet, anesthetized mice were perfused with 10 ml of PBS via left ventricle, followed by 10 ml of 10% buffered formalin phosphate. After removal of the adventitia, the aorta was opened longitudinally, pinned flat onto a black-wax plate and stained with oil red O (Sigma) as previously described[20]. Plaques were analyzed under the Zeiss stemi 200-C microscope connected to an Olympus BX41 digital camera, and the lesions were quantified with Image J analysis software. To analyze atherosclerosis in the outflow tract and valve area of the heart, top half of the heart was embedded in freezing media and stored at −80 °C until sectioning. Serial 10-μm-thick cryosections were cut and stained with hematoxylin and eosin as well as oil red O for quantifications of the lesion areas with the Image J analysis software. The aortic lesion size of each animal was obtained by the average in six sections from the same mice[20].

Isolation and Culture of Primary Endothelial Cells

Primary endothelial cells were isolated from the lungs of male *Pparγ*$^{F/F}$/*Ldlr*$^{-/-}$ or *Pparγ*$^{\Delta EC}$/*Ldlr*$^{-/-}$ mice. The mice were killed with carbon dioxide and the lungs were harvested and placed in DMEM. The tissues were trimmed, cut into small pieces and incubated at 37 °C with collagenase I (Invitrogen) for 45 minutes. The suspension was triturated with 30 cc syringe for 12 times, filtered through sterile 70 μm disposable cell strainer (BD Biosciences, San Jose, CA), and centrifuged at 400 *g* for 8 min. The cell pellet was resuspended in DPBS and incubated with dynabeads (Invitrogen) coated with anti-mouse CD31 antibody (BD Biosciences) on a rotator for 10 min at room temperature. The cell-bound beads were washed 5 times with DMEM and cultured in Medium 200 (Invitrogen) with the addition of Low Serum Growth Supplement (Invitrogen). Cells were grown in a collagen type I-coated plate and used at passage 2 for the experiments. The purification of ECs were > 90% as confirmed by CD31 immunofluoresence staining.

Monocyte-Endothelial Cell Adhesion Assay

Monocytes were isolated from C57/B6 mice as previously described[20] and labeled with calcein-AM (invitrogen). Confluent endothelial cells were treated with control or LPS for 16h and incubated with calcein-AM-labeled monocytes for 30 min. After washing with PBS for 3 times, monocytes bound to ECs were visualized on fluorescence microscopy. The

NIH-PA Author Manuscript

NIH-PA Author Manuscript

NIH-PA Author Manuscript

number of bound monocytes was quantified by counting 5 microscopic fields per well in triplicates.

In Vivo Vascular Permeability Assay

Six-week-old male *Pparγ*$^{F/F}$ or *Pparγ*$^{\Delta EC}$ were injected with Evans blue dye (EBD) (30 mg/kg in 100 μl normal saline). Mustard oil diluted to 5% in corn oil or vehicle (corn oil) was applied to the dorsal and ventral surfaces of the ear and photographs were taken 15 minutes after dye injection. After mice were euthanized, ears were removed, dry and weighted. EBD was extracted with 1 ml of formamide overnight at 55 °C and measured spectrophotometrically at 620 nm. Values were expressed as μg of dye/mg of ear tissue[25].

Immunohistochemistry

Snap-frozen fixed aortic rings embedded in OCT were sectioned, fixed in 10% buffered formalin phosphate and processed for antibody staining according to standard protocols. The following antibodies were used: anti-CD31 (BD Bioscience, San Jose, CA), F4/80 (Serotec, Raleigh, NC), VCAM-1 and ICAM-1 (R&D System, Minneapolis, MN). Positive cells and total cells were quantified of the aortic arch (five different sections) from four different mice of each genotyping using IMAGE J software.

RNA Analysis

Total RNA was extracted from aortas, liver or primary endothelial cells using Trizol reagent (Invitrogen, Carlsbad, CA) and further purified by RNeasy columns (QIAGEN, Valencia, CA). Quantitative real-time PCR (qPCR) were performed using cDNA generated from 1 μg total RNA with SuperScript II Reverse Transcriptase kit (Invitrogen). qPCR reactions were performed by use of SYBR green PCR master mix (Applied Biosystems, Foster City, CA) in an ABI Prism 7900HT sequence detection system (Applied Biosystems). Values were quantified by the comparative CT method and normalized to β-actin. Sequences for primers used to quantify mRNA are listed in Supplemental Table 1.

Data analysis

Results are expressed as means ± SD. Statistical analysis was performed using the Student *t* test (2 groups) or One-way ANOVA with Bonferroni procedure for multiple comparison tests (≥ 3 groups) with GraphPad Prism 5 (GraphPad Software Inc, San Diego, CA). Value of $P < 0.05$ was considered statistically significant.

Results

Deletion of PPARγ by the Tie2-driven Cre Recombinase Accelerates the Initiation of Atherosclerosis in *Ldlr* $^{-/-}$ mice

To investigate the contribution of EC PPARγ in the development of atherosclerosis, *Pparγ*$^{\Delta EC}$/*Ldlr*$^{-/-}$ were generated by crossing *Pparγ*$^{\Delta EC}$ [18, 19] with *Ldlr*$^{-/-}$ mice. To verify tissue-specific PPARγ deficiency, genomic DNA recombination and mRNA levels were assessed in aorta, spleen, macrophage, liver, brown adipose tissue and white adipose tissue (Supplemental figure IA). Quantitative real-time RT-PCR (qPCR) showed that Tie2-Cre directs an efficient PPARγ disruption in endothelial cells and bone marrow-derived hematopoietic cells, but not in liver, BAT or WAT from *Pparγ*$^{\Delta EC}$/*Ldlr*$^{-/-}$ mice (Supplemental figure IB). These results are consistent with previous data, in which Southern blot analysis revealed recombination in spleen and endothelial cells[18].

Comprehensive analysis of atherosclerotic lesions was performed. Atherosclerotic plaques were not observed in *PPARγ*$^{\Delta EC}$/*Ldlr*$^{+/+}$ on high-cholesterol diet for 4 weeks

NIH-PA Author Manuscript

NIH-PA Author Manuscript

NIH-PA Author Manuscript

(Supplemental figure IIA) or *Pparγ*$^{\Delta EC}$/*Ldlr*$^{-/-}$ mice on standard chow diet for 26 weeks (Supplemental figure IIB). To investigate the role of EC PPARγ in the initiation and early stage of atherosclerosis, *Pparγ*$^{\Delta EC}$/*Ldlr*$^{-/-}$ mice and littermate controls were challenged with high-cholesterol diet for 4 weeks. Atherosclerotic plaques were clearly visible by light microscopy in the aortic arch, innominate artery, left carotid artery, left subclavian artery, thoracic aorta, and abdominal aorta in *Pparγ*$^{\Delta EC}$/*Ldlr*$^{-/-}$ mice. However, no visual lesions were observed in the thoracic or abdominal aorta with any littermate controls. En face analysis of atheromatous plaques by oil red O staining showed a marked increase of plaques in the aorta from *Pparγ*$^{\Delta EC}$/*Ldlr*$^{-/-}$ mice when compared to control littermates (Figure 1A and 1B). Quantification of atherosclerotic lesions relative to aortic area revealed a dramatic increase of lesions in the aortic arch (Figure 1C), thoracic aorta (Figure 1D) as wells as abdominal aorta (Figure 1E) in *Pparγ*$^{\Delta EC}$/*Ldlr*$^{-/-}$ mice. Histological assessment of atherosclerotic lesions at the aortic sinus by H&E staining confirmed the results of en face analysis, revealing an increase of plaque formation in *Pparγ*$^{\Delta EC}$/*Ldlr*$^{-/-}$ mice compared to their *Pparγ*$^{F/F}$/*Ldlr*$^{-/-}$ littermate controls (Figure 1F). Similarly, there was a significant increase of lipid-burden plaque area in *Pparγ*$^{\Delta EC}$/*Ldlr*$^{-/-}$ mice compared with their littermate controls as revealed by oil red O staining on cross-sectional aorta sinus (Figure 1G). These data demonstrate an accelerated atherogenesis in *Pparγ*$^{\Delta EC}$/*Ldlr*$^{-/-}$ mice, suggesting an important role for endothelial PPARγ in protecting against atherogenesis.

Deficiency of PPARγ in EC Accelerates the Initiation of Atherosclerosis in *Ldlr*$^{-/-}$ mice

Recent studies demonstrate that Tie2 is expressed in 20% of human blood monocytes[26]. To test whether a PPARγ-dependent mechanism in macrophages accounts for the accelerated atherogenesis in the *Pparγ*$^{\Delta EC}$/*Ldlr*$^{-/-}$ mice, mice with a conditional disruption of PPARγ in macrophages, were bred to the *Ldlr*$^{-/-}$ background (*Pparγ*$^{\Delta M\phi}$/*Ldlr*$^{-/-}$). Interestingly, as revealed by en face staining with aorta (Figure 2A), *Pparγ*$^{\Delta M\phi}$/*Ldlr*$^{-/-}$ mice on 4 weeks of high cholesterol diet did not develop an increase in atherosclerotic lesions compared to *Pparγ*$^{F/F}$/*Ldlr*$^{-/-}$ littermate control mice. Although a previous study showed that macrophage-specific PPARγ deficiency could increase atherosclerosis in *Ldlr*$^{-/-}$ mice challenged with 16 weeks of butterfat diet[5], our data suggested that disruption of PPARγ in macrophage might not be essential for the initiation of atherogenesis.

PPARγ is deleted in bone-marrow-derived hematopoietic cells by the Tie2-driven Cre recombinase [18, 19]. To further elucidate whether the large increase in atherogenesis in *Pparγ*$^{\Delta EC}$/*Ldlr*$^{-/-}$ mice was due to decreased PPARγ in hematopoietic cells, bone marrow transplantation was undertaken. Bone marrow from *Pparγ*$^{F/F}$/*Ldlr*$^{-/-}$ or *Pparγ*$^{\Delta EC}$/*Ldlr*$^{-/-}$ was transplanted into 6-week-old, lethally irradiated *Pparγ*$^{\Delta EC}$/*Ldlr*$^{-/-}$ or *Pparγ*$^{F/F}$/*Ldlr*$^{-/-}$ mice, respectively. Four weeks after transplantation, peripheral blood was collected confirming full reconstitution of donor hematopoietic cells in the recipient mice. (Figure 2B). Mice were fed high-cholesterol diet for 4 weeks following bone marrow transplantation. *Pparγ*$^{F/F}$/*Ldlr*$^{-/-}$ mice reconstituted with *Pparγ*$^{\Delta EC}$/*Ldlr*$^{-/-}$ bone marrow exhibited 3.4% ± 0.26% of lesion areas in aortic arch (Figure 2C, left panel) and 0.008 ± 0.003 mm^2 of lesion in cross sections (Figure 2D, left panel). However, *Pparγ*$^{\Delta EC}$/*Ldlr*$^{-/-}$ mice transplanted with *Pparγ*$^{F/F}$/*Ldlr*$^{-/-}$ bone marrow maintained larger lesion areas both in aortic arch (Figure 2C, 17.0% ± 0.90%) and in cross sections (Figure 2D, 0.079 ± 0.004 mm^2). These data suggest that loss of PPARγ in bone-marrow-derived hematopoietic cells could not account for the enhanced aortic atherosclerosis in *Pparγ*$^{\Delta EC}$/*Ldlr*$^{-/-}$ mice. These data indicate that EC dysfunction in host mice lacking PPARγ is likely a major cause of lesion initiation in *Pparγ*$^{\Delta EC}$/*Ldlr*$^{-/-}$ mice.

NIH-PA Author Manuscript

NIH-PA Author Manuscript

NIH-PA Author Manuscript

Deficiency of PPARγ in EC Increases Serum Cholesterol and Triglycerides Following High-cholesterol Diet

Multiple metabolic parameters were assessed following high-cholesterol diet administration. No changes in body weights were observed between *Pparγ*$^{\Delta EC}$/*Ldlr*$^{-/-}$ and littermate control mice on standard chow or high-cholesterol diet (Figure 3A). At one week of high cholesterol feeding, both genotypes developed dyslipidemia (Figure 3B). *Pparγ*$^{\Delta EC}$/*Ldlr*$^{-/-}$ mice manifested more marked accumulation of serum cholesterol (Figure 3C, 2880 ± 572 *vs* 1420 ± 139 mg/dL) and TG (Figure 3D, 1170 ± 209 *vs* 732 ± 171 mg/dL) than *Pparγ*$^{F/F}$/*Ldlr*$^{-/-}$ controls. Cholesterol concentrations were also measured in lipoprotein fractions separated by fast protein liquid chromatography (FPLC). *Pparγ*$^{\Delta EC}$/*Ldlr*$^{-/-}$ mice exhibited more VLDL and LDL than *Pparγ*$^{F/F}$/*Ldlr*$^{-/-}$ mice (Figure 3E). Previous studies indicated that PPARγ in the endothelium regulates the metabolic response to high fat diet in mice[18,19]. In primary ECs isolated from *Pparγ*$^{\Delta EC}$/*Ldlr*$^{-/-}$ mice, a series of known PPARγ target genes involved in cholesterol and triglyceride metabolism were analyzed. No changes were found in mRNA expression of ABCA1 and ABCG1, which are known as cholesterol reverse transporters. However, CD36, a long-chain fatty acid receptor that facilitates fatty acid uptake, was significant decreased in ECs from *Pparγ*$^{\Delta EC}$/*Ldlr*$^{-/-}$ mice. Fatty acid binding protein 4 (Fabp4) was also repressed in the PPARγ-deficient ECs (Figure 3F).

EC PPARγ Disruption Is Associated with Increased Blood Pressure after High Cholesterol Diet Feeding

Since hypertension is a major risk factor for atherosclerosis, systolic blood pressure was analyzed using tail-cuff plethysmography. Without high cholesterol diet challenge, there was no significant difference between *Pparγ*$^{\Delta EC}$/*Ldlr*$^{-/-}$ (124 ± 6.2 mmHg) and *Pparγ*$^{F/F}$/*Ldlr*$^{-/-}$ (120 ± 3.4 mmHg). High cholesterol diet feeding increased systolic BP in both groups, however, *Pparγ*$^{\Delta EC}$/*Ldlr*$^{-/-}$ mice showed a higher mean systolic BP compared with their littermate controls (Table 1). This is consistent with our previously data showing that PPARγ deficiency in EC does not influence basal blood pressure but augments high fat diet-induced hypertension[18]. Measurement of AngII type 1 receptor (AT_1R) and eNOS mRNAs in the aortas from mice on standard chow diet or high cholesterol diet revealed no statistical difference in levels between *Pparγ*$^{F/F}$/*Ldlr*$^{-/-}$ and *Pparγ*$^{\Delta EC}$/*Ldlr* $^{-/-}$ mice on standard chow diet. When challenged with a high cholesterol diet, an increase of AT_1R mRNA was detected in *Pparγ*$^{\Delta EC}$/*Ldlr*$^{-/-}$ mice compared to their littermate controls. However, no changes of eNOS mRNA was detected between these two groups (Supplemental figure III).

Disruption of EC PPARγ Increases Endothelial Permeability

It has been hypothesized that the dysfunction of ECs is an important early event for the development of atherosclerosis [8, 9] and the sites of plaque development may be associated with impaired EC functions. To determine the potential mechanisms of enhanced atherosclerosis in the *Pparγ*$^{\Delta EC}$/*Ldlr*$^{-/-}$ mice, endothelial barrier function in the mice was assessed. Leakage of Evans Blue dye into interstitial tissues of the mouse ear after treatment with mustard oil directly correlates to impaired endothelial barrier function. *Pparγ*$^{\Delta EC}$ mice exhibited a significantly higher degree of vascular leakage when compared to *Pparγ*$^{F/F}$ mice (Figure 4A and B, 46.8 ± 9.09 μg/mg in *Pparγ*$^{F/F}$ versus 89.5± 17.4 in *Pparγ*$^{\Delta EC}$, $p<0.05$), indicating an impaired endothelial function after PPARγ deficiency. To elucidate the mechanisms of increased endothelial permeability by EC-*Pparγ* disruption, genes involved in adherens junctions and tight junctions were evaluated. No significant change was found in the mRNA levels of VE-cadherin, claudins, zonula occludens, or occludins (Figure 4C).

NIH-PA Author Manuscript

NIH-PA Author Manuscript

NIH-PA Author Manuscript

Increased inflammation and macrophage infiltration by *Pparγ* disruption in vitro and in vivo

A significant increase in endothelial permeability was observed after disruption of PPARγ in EC. Since no direct transcriptionally mediators were identified, inflammation was assessed. Pro-inflammatory mediators were shown to be direct repressive targets of PPARγ [27, 28] and increased inflammation is a major mechanism leading to endothelial barrier dysfunction [28, 29]. To understand the mechanism by which ECs are activated, primary ECs were used and the expression patterns of proinflammatory genes were analyzed. PPARγ-deficient ECs exhibited higher expression of inflammatory chemokines and adherent molecules, such as MCP-1, ICAM-1 and VCAM-1, which are important for monocyte recruitment and interaction with endothelium. Interestingly, iNOS, a key mediator critical for inflammation and barrier permeability, was dramatically increased after EC-*Pparγ* disruption. Moreover, the expression of the above genes was further extended in response to LPS treatment for 16 h (Figure 5A). Next, EC-monocyte adhesion assays were performed to determine the recruitment of monocytes to activated ECs. *Pparγ* disruption markedly increased the primary monocyte adhesion to ECs under basal level, and pre-administration of LPS augmented the recruitment and adhesion of monocytes to ECs (Figure 5B). These data demonstrated an activated phenotype of ECs by *Pparγ* loss-of-function in ECs *in vitro*. Activation of ECs was further assessed by analysis of mRNAs encoding inflammatory modulators in the vessel wall of $Pparγ^{\Delta EC}/Ldlr^{-/-}$ mice after high cholesterol diet treatment. Consistent with *in vitro* data, several inflammatory molecules, MCP-1, iNOS and TNFα, were significantly upregulated in the $Pparγ^{\Delta EC}/Ldlr^{-/-}$ mice compared to $Pparγ^{F/F}/Ldlr^{-/-}$. VCAM-1, which is expressed after the activation of endothelial cells and mediates the adhesion of leukocytes, was also significantly increased in $Pparγ^{\Delta EC}/Ldlr^{-/-}$ aorta (Figure 5C). In addition, the expression of VCAM-1 and macrophage marker F4/80 was examined in aortic roots by immunofluorescent staining. $Pparγ^{\Delta EC}/Ldlr^{-/-}$ mice demonstrated a greater area positive for VCAM-1 and F4/80 (Figure 5D), indicating an exacerbated macrophage infiltration and inflammation after PPARγ disruption in endothelial cells.

Discussion

Atherosclerosis is as a complex disease due to the formation of atherosclerotic lesions consisting of accumulated modified lipids, VSMCs, ECs, leukocytes and foam cells[30, 31]. PPARγ is highly expressed in both the normal vasculature, including ECs, VSMCs, and macrophages[17, 32, 33], and in atherosclerotic plaques[34]. Several studies were performed to investigate the role of PPARγ in the development of atherosclerosis. In macrophage, loss of PPARγ leads to reduced cholesterol efflux and decreased expression of lipoprotein lipase, liver X receptor, and ABCG1[17]. Transplantation of PPARγ-deficient macrophage[5, 35] into $Ldlr^{-/-}$ mice resulted in significant increase of atherosclerotic lesion. Others showed that PPARγ deficiency in VSMC specifically could augment angtension II-induced atherosclerosis without affecting abdominal aortic aneurysms[6]. While these studies demonstrated a beneficial effect of PPARγ in more advanced stages of atherosclerotic lesions, little is known about the role of PPARγ in the initiation of atherosclerosis.

The present study demonstrated that PPARγ in endothelial cells is a critical player in protecting against the development of atherosclerosis, especially the initiation of atherogenesis using a loss-of-function strategy. $Ldlr^{-/-}$ mice with EC-specific disruption of PPARγ develop atherosclerosis as early as 4 weeks on a high cholesterol diet, suggesting an important vascular protective role of endothelial PPARγ against atherogenesis. Mechanistically, disruption of EC PPARγ leads to an increase of several pro-atherosclerotic pathways including exacerbated dyslipidemia, raised systolic blood pressure, increased

NIH-PA Author Manuscript

NIH-PA Author Manuscript

NIH-PA Author Manuscript

endothelial permeability, enhanced expression of proinflammatory cytokines, and increased monocyte/macrophage recruitment and infiltration into vessel walls.

ECs serve as an important barrier between vascular tissue and blood components as well as modulate the traffic of immune cells. Its activation upon exposure to cardiovascular risk factors, such as hyperglycemia, hypercholesterolemia, hypertension, and smoking is the first step of atherogenesis[36]. Disruption of PPARγ in ECs exacerbates dyslipidemia in *Ldlr*$^{-/-}$ mice. Defective cholesterol and triglyceride metabolism in EC after PPARγ disruption might contribute to the large increases in serum lipid concentrations. A previous study showed PPARγ in endothelial cells regulates metabolic responses to high fat diet in mice, in which defective fatty acid uptake and triglyceride metabolism occurred only in the absence of EC PPARγ [19]. The data in the present manuscript further confirms the role of EC PPARγ in regulation of lipid homeostasis.

Hypertension is a major risk factor for atherosclerosis and cardiovascular disease. The current study showed that PPARγ disruption in EC raised systolic BP after a high cholesterol diet challenge. In addition, AT1R mRNA was also significantly upregulated, suggesting an impaired vascular activity. Others revealed that PPARγ disruption in EC is associated with impaired vascular relaxation after a high fat diet in which carotid artery dilation response to carbachol was measured after phenylephrine preconstriction[19]. It addition, it has demonstrated an increased contraction in aortic rings from PPARγ KO mice[37]. These data support the current study of endothelial dysfunction and increased BP in *Pparγ*$^{\Delta EC}$ mice.

Deficiency of EC PPARγ dramatically upregulated several proinflammtory molecules, such as vascular adhesion molecule-1 (VCAM-1), intercellular adhesion molecule-1 (ICAM-1), monocyte chemoattractant protein-1 (MCP-1) and TNFα in the vessel wall, all of which are critical for the recruitment, rolling, and trafficking of monocytes into subendothelium. This result is consistent with in vitro studies showing that PPARγ activation by its ligands inhibits proinflammatory cytokines and chemokines in ECs[12, 38, 39]. Recently, bioinformatics analysis of gene sets regulated by ligand-activated and dominant-negative PPARγ in the mouse aorta is consistent with the present study. VCAM-1, ICAM-1, MCP-1, and TNFα mRNA expression were repressed by PPARγ ligand rosiglitazone and induced by PPARγ P465L dominant-negative mutation[40].

Disruption of PPARγ in EC significantly raised vascular permeability as demonstrated by Evans Blue leakage assay. While no transcriptional changes of barrier genes were observed, dyslipidemia and increased inflammation that are found in the result in impaired barrier function of ECs. Inflammation and iNOS can increase barrier permeability in EC[41], consistent with the present results showing increased proinflammatory cytokines, chemokines, and iNOS in *Pparγ*$^{\Delta EC}$ mouse ECs that have elevated vascular permeability.

The present study demonstrates PPARγ deficiency in EC leads to multiple endothelial dysfunctions in *Ldlr*$^{-/-}$ mice exposed to high cholesterol diet. Although further study is needed to explore which is the first step in this process, the current study provides first definitive evidence that endothelial PPARγ serves as a critical player for protecting against the initiation of atherosclerosis using EC-specific PPARγ disruption animal models and thus raises a potentially clinical therapeutic strategy to prevent atherogenesis.

Supplementary Material

Refer to Web version on PubMed Central for supplementary material.

NIH-PA Author Manuscript

NIH-PA Author Manuscript

NIH-PA Author Manuscript

Acknowledgments

We thank Dr. Jeffrey Kopp for advice and the use of a plethysmographic apparatus for blood pressure measurements.

Funding sources

This work was supported by the National Cancer Institute Intramural Research Program and National Institutes of Health Grant CA148828 (to YMS).

References

1. Tontonoz P, Spiegelman BM. Fat and beyond: The diverse biology of ppargamma. Annu Rev Biochem. 2008; 77:289–312. [PubMed: 18518822]
2. Li AC, Brown KK, Silvestre MJ, Willson TM, Palinski W, Glass CK. Peroxisome proliferator-activated receptor γ ligands inhibit development of atherosclerosis in ldl receptor-deficient mice. J Clin Invest. 2000; 106:523–531. [PubMed: 10953027]
3. Collins AR, Meehan WP, Kintscher U, Jackson S, Wakino S, Noh G, Palinski W, Hsueh WA, Law RE. Troglitazone inhibits formation of early atherosclerotic lesions in diabetic and nondiabetic low density lipoprotein receptor-deficient mice. Arterioscler Thromb Vasc Biol. 2001; 21:365–371. [PubMed: 11231915]
4. Chen Z, Ishibashi S, Perrey S, Osuga J, Gotoda T, Kitamine T, Tamura Y, Okazaki H, Yahagi N, Iizuka Y, Shionoiri F, Ohashi K, Harada K, Shimano H, Nagai R, Yamada N. Troglitazone inhibits atherosclerosis in apolipoprotein e-knockout mice: Pleiotropic effects on cd36 expression and hdl. Arterioscler Thromb Vasc Biol. 2001; 21:372–377. [PubMed: 11231916]
5. Babaev VR, Yancey PG, Ryzhov SV, Kon V, Breyer MD, Magnuson MA, Fazio S, Linton MF. Conditional knockout of macrophage PPARγ increases atherosclerosis in c57bl/6 and low-density lipoprotein receptor-deficient mice. Arterioscler Thromb Vasc Biol. 2005; 25:1647–1653. [PubMed: 15947238]
6. Subramanian V, Golledge J, Ijaz T, Bruemmer D, Daugherty A. Pioglitazone-induced reductions in atherosclerosis occur via smooth muscle cell-specific interaction with PPARγ. Circ Res. 2010; 107:953–958. [PubMed: 20798360]
7. Hamblin M, Chang L, Zhang H, Yang K, Zhang J, Chen YE. Vascular smooth muscle cell peroxisome proliferator-activated receptor–γ mediates pioglitazone-reduced vascular lesion formation. Arterioscler Thromb Vasc Biol. 2011; 31:352–359. [PubMed: 21088248]
8. Littlewood TD, Bennett MR. Apoptotic cell death in atherosclerosis. Curr Opin Lipidol. 2003; 14:469–475. [PubMed: 14501585]
9. Tricot O, Mallat Z, Heymes C, Belmin J, Leseche G, Tedgui A. Relation between endothelial cell apoptosis and blood flow direction in human atherosclerotic plaques. Circulation. 2000; 101:2450–2453. [PubMed: 10831515]
10. Delerive P, Martin-Nizard F, Chinetti G, Trottein F, Fruchart JC, Najib J, Duriez P, Staels B. Peroxisome proliferator-activated receptor activators inhibit thrombin-induced endothelin-1 production in human vascular endothelial cells by inhibiting the activator protein-1 signaling pathway. Circ Res. 1999; 85:394–402. [PubMed: 10473669]
11. Diep QN, El Mabrouk M, Cohn JS, Endemann D, Amiri F, Virdis A, Neves MF, Schiffrin EL. Structure, endothelial function, cell growth, and inflammation in blood vessels of angiotensin ii-infused rats: Role of peroxisome proliferator-activated receptor-γ. Circulation. 2002; 105:2296–2302. [PubMed: 12010913]
12. Wang N, Verna L, Chen NG, Chen J, Li H, Forman BM, Stemerman MB. Constitutive activation of peroxisome proliferator-activated receptor-γ suppresses pro-inflammatory adhesion molecules in human vascular endothelial cells. J Biol Chem. 2002; 277:34176–34181. [PubMed: 12107164]
13. Ptasinska A, Wang S, Zhang J, Wesley RA, Danner RL. Nitric oxide activation of peroxisome proliferator-activated receptor γ through a p38 mapk signaling pathway. FASEB J. 2007; 21:950–961. [PubMed: 17197391]
14. Duan SZ, Usher MG, Mortensen RM. Peroxisome proliferator-activated receptor-γ-mediated effects in the vasculature. Circ Res. 2008; 102:283–294. [PubMed: 18276926]

NIH-PA Author Manuscript NIH-PA Author Manuscript NIH-PA Author Manuscript

15. Dormandy JA, Charbonnel B, Eckland DJ, Erdmann E, Massi-Benedetti M, Moules IK, Skene AM, Tan MH, Lefebvre PJ, Murray GD, Standl E, Wilcox RG, Wilhelmsen L, Betteridge J, Birkeland K, Golay A, Heine RJ, Koranyi L, Laakso M, Mokan M, Norkus A, Pirags V, Podar T, Scheen A, Scherbaum W, Schernthaner G, Schmitz O, Skrha J, Smith U, Taton J. Secondary prevention of macrovascular events in patients with type 2 diabetes in the proactive study (prospective pioglitazone clinical trial in macrovascular events): A randomised controlled trial. Lancet. 2005; 366:1279–1289. [PubMed: 16214598]
16. Nissen SE, Wolski K. Effect of rosiglitazone on the risk of myocardial infarction and death from cardiovascular causes. N Engl J Med. 2007; 356:2457–2471. [PubMed: 17517853]
17. Akiyama TE, Sakai S, Lambert G, Nicol CJ, Matsusue K, Pimprale S, Lee YH, Ricote M, Glass CK, Brewer HB Jr, Gonzalez FJ. Conditional disruption of the peroxisome proliferator-activated receptor γ gene in mice results in lowered expression of abca1, abcg1, and apoe in macrophages and reduced cholesterol efflux. Mol Cell Biol. 2002; 22:2607–2619. [PubMed: 11909955]
18. Nicol CJ, Adachi M, Akiyama TE, Gonzalez FJ. PPARγ in endothelial cells influences high fat diet-induced hypertension. Am J Hypertens. 2005; 18:549–556. [PubMed: 15831367]
19. Kanda T, Brown JD, Orasanu G, Vogel S, Gonzalez FJ, Sartoretto J, Michel T, Plutzky J. PPARγ in the endothelium regulates metabolic responses to high-fat diet in mice. J Clin Invest. 2009; 119:110–124. [PubMed: 19065047]
20. Shah YM, Morimura K, Gonzalez FJ. Expression of peroxisome proliferator-activated receptor-γ in macrophage suppresses experimentally induced colitis. Am J Physiol Gastrointest Liver Physiol. 2007; 292:G657–666. [PubMed: 17095756]
21. Ordovas JM, Osgood D. Preparative isolation of plasma lipoproteins using fast protein liquid chromatography (fplc). Methods Mol Biol. 1998; 110:105–111. [PubMed: 9918042]
22. Innis-Whitehouse W, Li X, Brown WV, Le NA. An efficient chromatographic system for lipoprotein fractionation using whole plasma. J Lipid Res. 1998; 39:679–690. [PubMed: 9548599]
23. Linton MF, Atkinson JB, Fazio S. Prevention of atherosclerosis in apolipoprotein e-deficient mice by bone marrow transplantation. Science. 1995; 267:1034–1037. [PubMed: 7863332]
24. Fazio S, Linton MF. Murine bone marrow transplantation as a novel approach to studying the role of macrophages in lipoprotein metabolism and atherogenesis. Trends Cardiovasc Med. 1996; 6:58–65. [PubMed: 21232276]
25. Thurston G, Suri C, Smith K, McClain J, Sato TN, Yancopoulos GD, McDonald DM. Leakage-resistant blood vessels in mice transgenically overexpressing angiopoietin-1. Science. 1999; 286:2511–2514. [PubMed: 10617467]
26. Murdoch C, Tazzyman S, Webster S, Lewis CE. Expression of tie-2 by human monocytes and their responses to angiopoietin-2. J Immunol. 2007; 178:7405–7411. [PubMed: 17513791]
27. Pascual G, Sullivan AL, Ogawa S, Gamliel A, Perissi V, Rosenfeld MG, Glass CK. Anti-inflammatory and antidiabetic roles of PPARγ. Novartis Found Symp. 2007; 286:183–196. [PubMed: 18269183]
28. Fu P, Birukov KG. Oxidized phospholipids in control of inflammation and endothelial barrier. Transl Res. 2009; 153:166–176. [PubMed: 19304275]
29. Kumar P, Shen Q, Pivetti CD, Lee ES, Wu MH, Yuan SY. Molecular mechanisms of endothelial hyperpermeability: Implications in inflammation. Expert Rev Mol Med. 2009; 11:e19. [PubMed: 19563700]
30. Libby P. Inflammation in atherosclerosis. Nature. 2002; 420:868–874. [PubMed: 12490960]
31. Galkina E, Ley K. Immune and inflammatory mechanisms of atherosclerosis. Annu Rev Immunol. 2009; 27:165–197. [PubMed: 19302038]
32. Law RE, Goetze S, Xi XP, Jackson S, Kawano Y, Demer L, Fishbein MC, Meehan WP, Hsueh WA. Expression and function of ppargamma in rat and human vascular smooth muscle cells. Circulation. 2000; 101:1311–1318. [PubMed: 10725292]
33. Marx N, Schonbeck U, Lazar MA, Libby P, Plutzky J. Peroxisome proliferator-activated receptor γ activators inhibit gene expression and migration in human vascular smooth muscle cells. Circ Res. 1998; 83:1097–1103. [PubMed: 9831704]
34. Ricote M, Huang J, Fajas L, Li A, Welch J, Najib J, Witztum JL, Auwerx J, Palinski W, Glass CK. Expression of the peroxisome proliferator-activated receptor γ (PPARγ) in human atherosclerosis

NIH-PA Author Manuscript

NIH-PA Author Manuscript

NIH-PA Author Manuscript

and regulation in macrophages by colony stimulating factors and oxidized low density lipoprotein. Proc Natl Acad Sci U S A. 1998; 95:7614–7619. [PubMed: 9636198]

35. Chawla A, Boisvert WA, Lee CH, Laffitte BA, Barak Y, Joseph SB, Liao D, Nagy L, Edwards PA, Curtiss LK, Evans RM, Tontonoz P. A PPARγ-LXR-ABCA1 pathway in macrophages is involved in cholesterol efflux and atherogenesis. Mol Cell. 2001; 7:161–171. [PubMed: 11172721]
36. Tesfamariam B, DeFelice AF. Endothelial injury in the initiation and progression of vascular disorders. Vascul Pharmacol. 2007; 46:229–237. [PubMed: 17218160]
37. Yuen CY, Wong WT, Tian XY, Wong SL, Lau CW, Yu J, Tomlinson B, Yao X, Huang Y. Telmisartan inhibits vasoconstriction via PPARγ-dependent expression and activation of endothelial nitric oxide synthase. Cardiovasc Res. 2011; 90:122–129. [PubMed: 21156825]
38. Pasceri V, Wu HD, Willerson JT, Yeh ET. Modulation of vascular inflammation in vitro and in vivo by peroxisome proliferator-activated receptor-gamma activators. Circulation. 2000; 101:235–238. [PubMed: 10645917]
39. Jackson SM, Parhami F, Xi XP, Berliner JA, Hsueh WA, Law RE, Demer LL. Peroxisome proliferator-activated receptor activators target human endothelial cells to inhibit leukocyte-endothelial cell interaction. Arterioscler Thromb Vasc Biol. 1999; 19:2094–2104. [PubMed: 10479650]
40. Keen HL, Halabi CM, Beyer AM, de Lange WJ, Liu X, Maeda N, Faraci FM, Casavant TL, Sigmund CD. Bioinformatic analysis of gene sets regulated by ligand-activated and dominant-negative peroxisome proliferator-activated receptor γ in mouse aorta. Arterioscler Thromb Vasc Biol. 2010; 30:518–525. [PubMed: 20018933]
41. Komarova Y, Malik AB. Regulation of endothelial permeability via paracellular and transcellular transport pathways. Annu Rev Physiol. 2010; 72:463–493. [PubMed: 20148685]

NIH-PA Author Manuscript

NIH-PA Author Manuscript

NIH-PA Author Manuscript

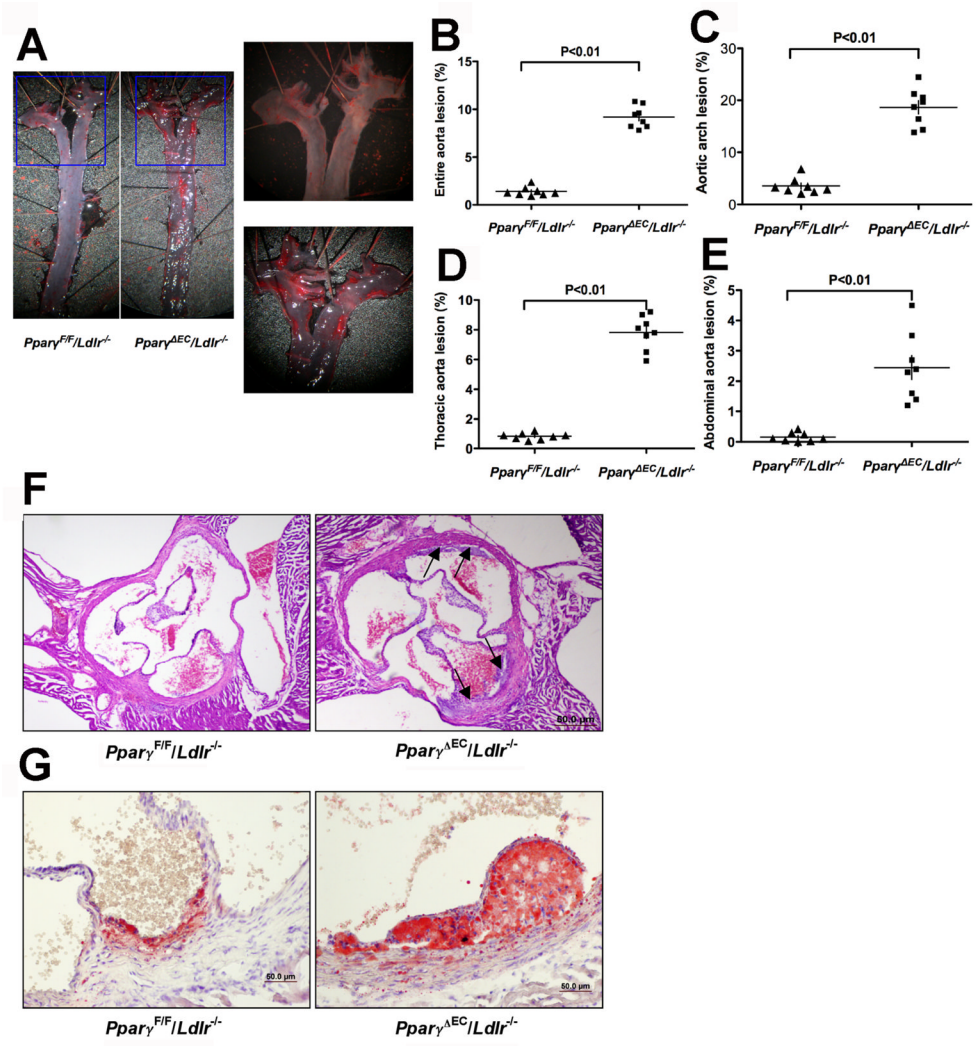

Figure 1. Deficiency of PPARγ in ECs accelerates atherogenesis in *Ldlr*$^{-/-}$ mice

Pparγ$^{F/F}$/*Ldlr*$^{-/-}$ and *Pparγ*$^{\Delta EC}$/*Ldlr*$^{-/-}$ mice consumed a high cholesterol diet for 4 weeks and underwent analysis of lesion size in the aorta and aortic root.

A. Representative images of entire aortas stained with oil red O for lipid deposition. B-E. Quantification of lesion area for entire aorta (B), aortic arch (C), thoracic aorta (D) and abdominal aorta (E), respectively. All the quantification was expressed as % of corresponding area. *P<0.05 and **P<0.01 *versus PPARγ*$^{F/F}$/*Ldlr*$^{-/-}$ group (n=8).

F. Representative examples of cross-sections from the aortic root stained with H.E. Black arrows indicate atherosclerotic lesions.

G. Representative examples of cross-sections from the aortic root stained with oil red O to show the lipid deposition.

NIH-PA Author Manuscript

NIH-PA Author Manuscript

NIH-PA Author Manuscript

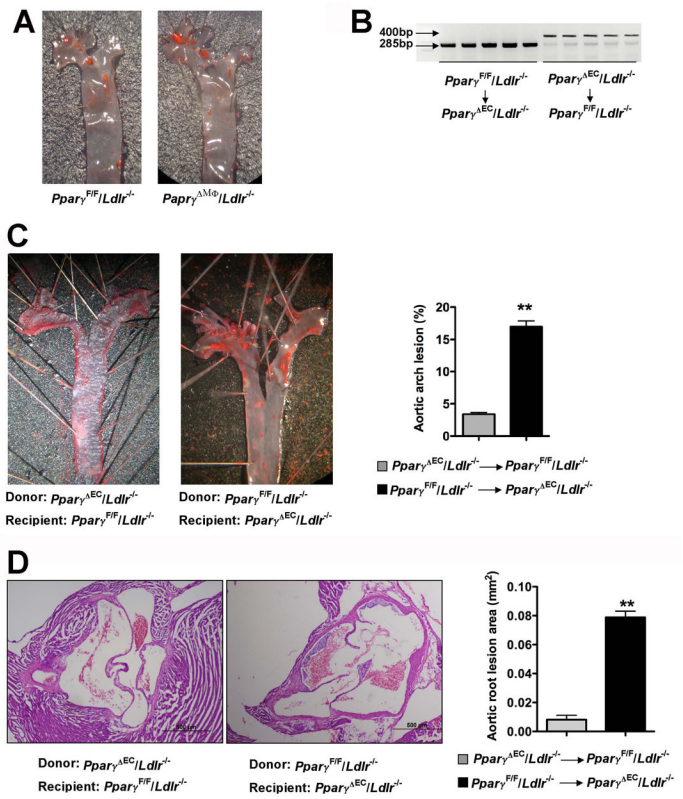

Figure 2. Bone marrow transplantation does not change the host atherosclerotic phenotypes

A. Oil red O staining showing atherosclerotic lesions for aortic arch from $Ppar\gamma^{\Delta M\phi}/Ldlr^{-/-}$ mice. Mice were fed a high cholesterol diet and aortic arch was dissected for en face oil red O staining.

B. PCR analysis for *Pparγ* alleles of peripheral blood from irradiated $Ppar\gamma^{F/F}/Ldlr^{-/-}$ mice transplanted with $Ppar\gamma^{\Delta EC}/Ldlr^{-/-}$ bone marrow or from irradiated $Ppar\gamma^{\Delta EC}/Ldlr^{-/-}$ mice transplanted with $Ppar\gamma^{F/F}/Ldlr^{-/-}$ bone marrow. DNA was extracted from 100 μl of peripheral blood 4 weeks after bone marrow transplantation. The PCR product for the $Ppar\gamma^{F/F}$ allele is 285 bp and for the $Ppar\gamma^{\Delta EC}$ allele is 400 bp

C. Lesion analysis in aorta from $Ppar\gamma^{F/F}/Ldlr^{-/-}$ mice transplanted with $Ppar\gamma^{\Delta EC}/Ldlr^{-/-}$ bone marrow or from $Ppar\gamma^{\Delta EC}/Ldlr^{-/-}$ mice transplanted with $Ppar\gamma^{F/F}/Ldlr^{-/-}$ bone marrow. Mice were treated with high cholesterol diet for 4 weeks after confirming fully chimerism and oil red O staining and quantification of lesion areas were performed.

D. Lesion area in the aortic root from $Ppar\gamma^{F/F}/Ldlr^{-/-}$ mice transplanted with $Ppar\gamma^{\Delta EC}/Ldlr^{-/-}$ bone marrow or from $Ppar\gamma^{\Delta EC}/Ldlr^{-/-}$ mice transplanted with $Ppar\gamma^{F/F}/Ldlr^{-/-}$ bone marrow. **P<0.01.

NIH-PA Author Manuscript

NIH-PA Author Manuscript

NIH-PA Author Manuscript

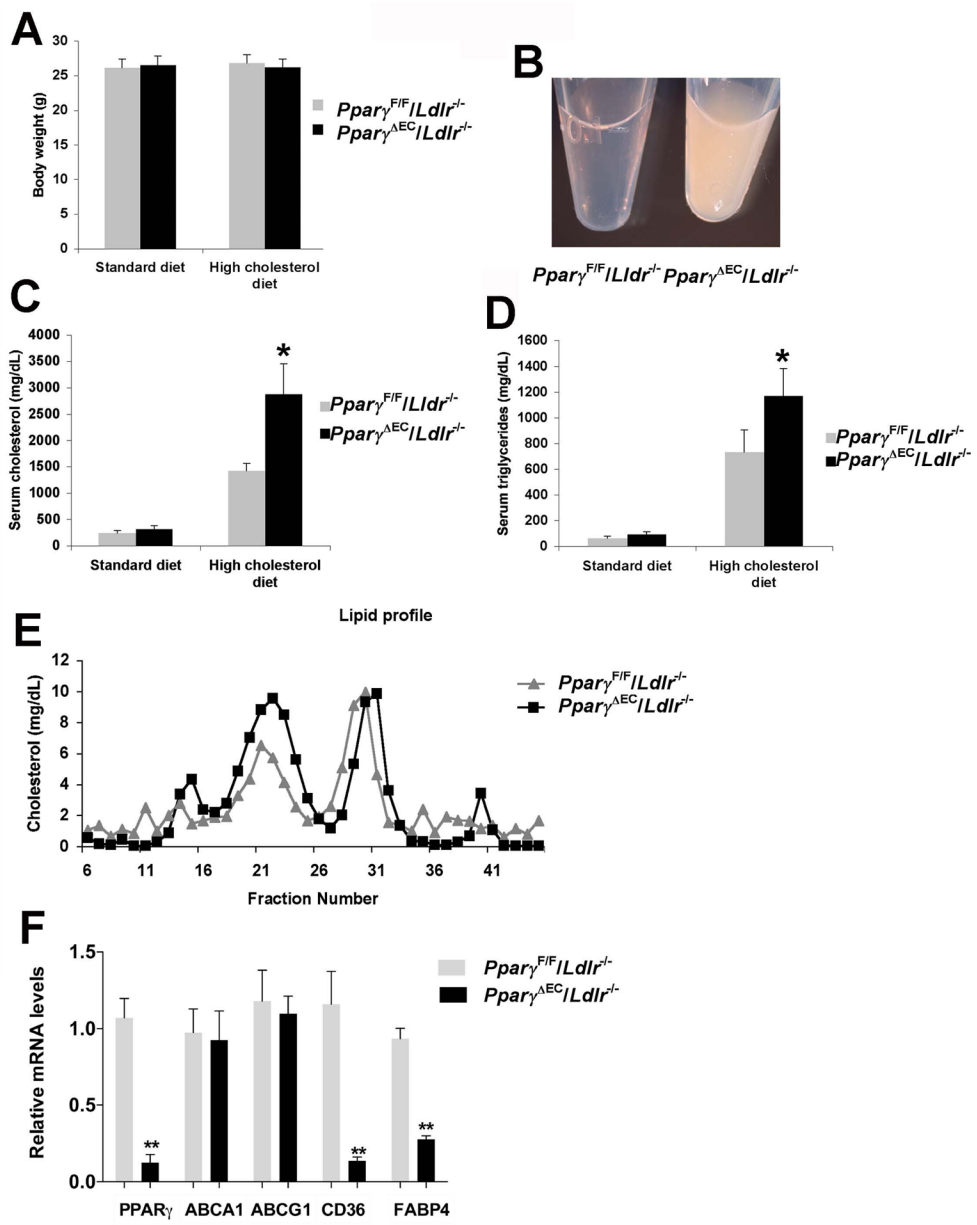

Figure 3. Exacerbated dyslipidemia in absence of EC PPARγ

A. Body weight of *Pparγ*$^{F/F}$/*Ldlr*$^{-/-}$ and *Pparγ*$^{\Delta EC}$/*Ldlr*$^{-/-}$ mice on standard diet or a high-cholesterol diet for 4 weeks.

B. Representative fasting serum from *Pparγ*$^{F/F}$/*Ldlr*$^{-/-}$ or *Pparγ*$^{\Delta EC}$/*Ldlr*$^{-/-}$ mice.

C. Fasting cholesterol levels of *Pparγ*$^{F/F}$/*Ldlr*$^{-/-}$ or *Pparγ*$^{\Delta EC}$/*Ldlr*$^{-/-}$ mice before and after 4 weeks of high cholesterol diet.

D. Fasting triglycerides levels from both groups of mice before and after 4 weeks on a high cholesterol diet.

E. Lipoprotein profiles from *Pparγ*$^{F/F}$/*Ldlr*$^{-/-}$ or *Pparγ*$^{\Delta EC}$/*Ldlr*$^{-/-}$ mice after one week of high cholesterol diet. *P < 0.05 *versus* the littermate controls.

F. Expression of genes in ECs of *Pparγ*$^{\Delta EC}$/*Ldlr*$^{-/-}$ versus *Pparγ*$^{F/F}$/*Ldlr*$^{-/-}$ mice. n=5 per group. **P < 0.01 *versus* the littermate controls.

NIH-PA Author Manuscript

NIH-PA Author Manuscript

NIH-PA Author Manuscript

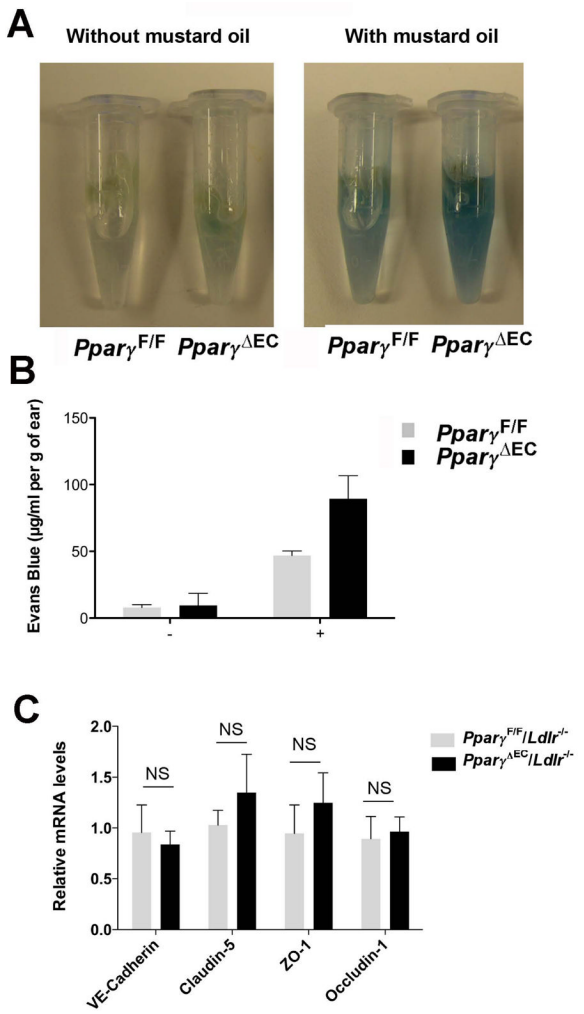

Figure 4. Increased permeability of endothelium in the absence of PPARγ

A. Photographs of ears after treatment with mustard oil (15 min) and vascular perfusion, showing relative amount of extravasated Evans blue tracer.

B. Spectrophotometric measurement of amount of extravasated Evans blue in mouse ears 15 min after topical application of mustard oil. *P<0.05 compared with controls.

C. Expression of genes related with adherens junctions and tight junctions in ECs. NS indicated no statistic difference.

NIH-PA Author Manuscript

NIH-PA Author Manuscript

NIH-PA Author Manuscript

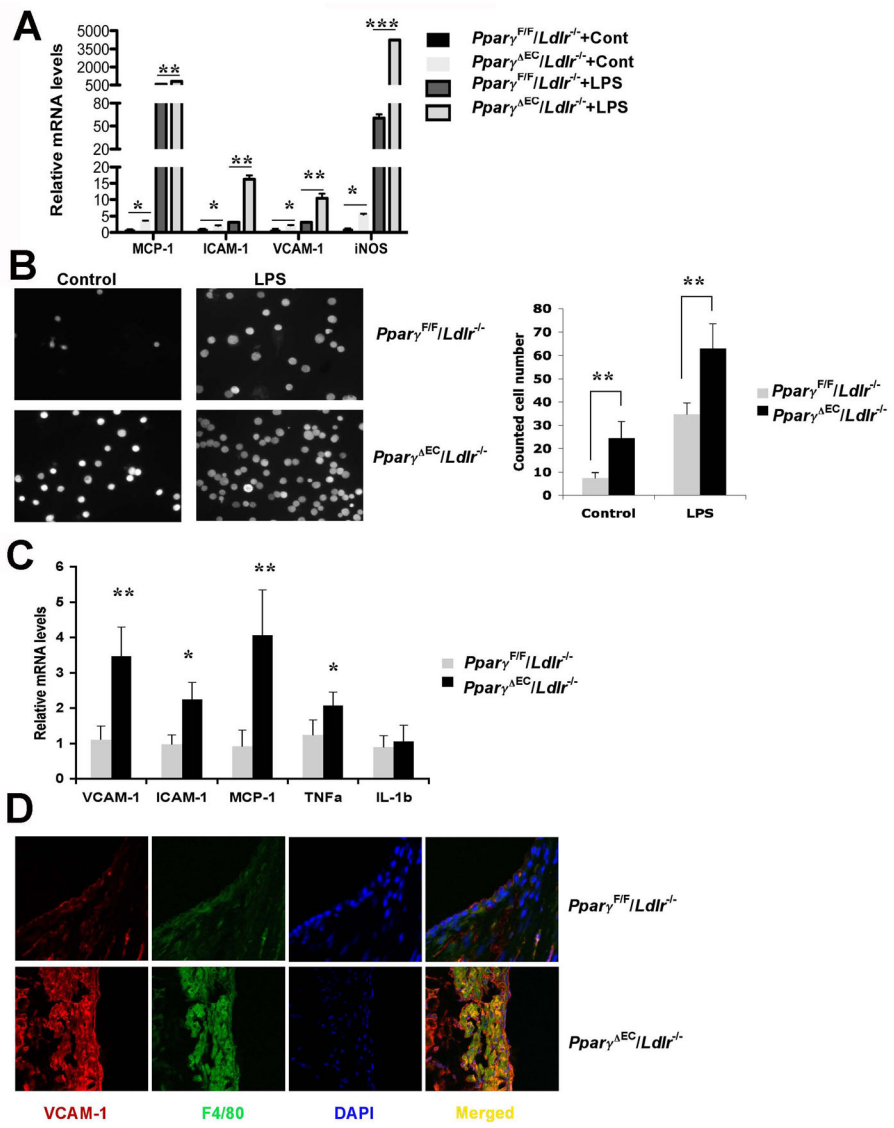

Figure 5. Lack of EC PPARγ leads to increased inflammation in vessel wall

A. qPCR analysis for mRNA levels of proinflammtory genes in primary ECs from *Pparγ*$^{F/F}$/*Ldlr*$^{-/-}$ or *Pparγ*$^{\Delta EC}$/*Ldlr*$^{-/-}$ mice with or without 100 ng/mL LPS treatment.

B. Endothelial-macrophage adhesion assay. Calcein AM-labeled primary macrophages bound to ECs were visualized on fluorescence microscopy. The number of bound macrophages was quantified by counting 5 microscopic fields per well in triplicates.

C. qPCR analysis for mRNA levels of proinflammatory genes in the whole aortas from *Pparγ*$^{F/F}$/*Ldlr*$^{-/-}$ or *Pparγ*$^{\Delta EC}$/*Ldlr*$^{-/-}$ mice with 4-week high-cholesterol diet challenge.

D. Representative examples of cross sections from the aortic sinus labeled for VCAM-1 and F4/80 (marker for macrophages), respectively. *P < 0.05, **P < 0.01 and ***P <0.001 *versus* the controls.

NIH-PA Author Manuscript
NIH-PA Author Manuscript
NIH-PA Author Manuscript

Table 1

Mean systolic BP for *Pparγ*$^{F/F}$/*Ldlr*$^{-/-}$ or *Pparγ*$^{\Delta EC}$/*Ldlr*$^{-/-}$ mice on high cholesterol diet

Group	0 week (mmHg)	1 week (mmHg)	4 weeks (mmHg)
Pparγ$^{F/F}$/*Ldlr*$^{-/-}$	120 ± 3.4	128 ± 3.2 *	134± 2.5**
Pparγ$^{\Delta EC}$/*Ldlr*$^{-/-}$	124 ± 6.2	139± 5.6†	149 ± 6.0††

0 week = standard chow diet; 1 week = 1 week treatment with high cholesterol diet; 4 weeks = 4 weeks of treatment with high cholesterol diet.

Mean values were calculated by averaging the last two-day values for each animal.

Values shown were means ± SEM. N=6 per group. *p<0.05 and **p<0.01 versus *Pparγ*$^{F/F}$/*Ldlr*$^{-/-}$ (0 weeks).

†p<0.05 versus *Pparγ*$^{F/F}$/*Ldlr*$^{-/-}$ (1 week) and

††p<0.01 versus *Pparγ*$^{F/F}$/*Ldlr*$^{-/-}$ (4 weeks).